

Received: 2013.08.23
Accepted: 2013.10.11
Published: 2014.01.13

Towards neural correlates of auditory stimulus processing: A simultaneous auditory evoked potentials and functional magnetic resonance study using an odd-ball paradigm

Authors' Contribution:
Study Design A
Data Collection B
Statistical Analysis C
Data Interpretation D
Manuscript Preparation E
Literature Search F
Funds Collection G

ABCDEF 1 **Rafał Milner**
ABCDEF 1 **Mateusz Rusiniak**
DEF 1 **Monika Lewandowska**
ABCDE 1 **Tomasz Wolak**
B 1 **Małgorzata Ganc**
ACD 2 **Ewa Piątkowska-Janko**
ACD 2 **Piotr Bogorodzki**
G 1 **Henryk Skarżyński**

1 World Hearing Center, Institute of Physiology and Pathology of Hearing, Warsaw/Kajetany, Poland
2 Nuclear and Medical Electronics Division, Institute of Radioelectronics, Warsaw University of Technology, Warsaw, Poland

Corresponding Author: Rafał Milner, e-mail: r.milner@ifps.org.pl
Source of support: The study was supported by grant MSHE no N403 214939

Background: The neural underpinnings of auditory information processing have often been investigated using the odd-ball paradigm, in which infrequent sounds (deviants) are presented within a regular train of frequent stimuli (standards). Traditionally, this paradigm has been applied using either high temporal resolution (EEG) or high spatial resolution (fMRI, PET). However, used separately, these techniques cannot provide information on both the location and time course of particular neural processes. The goal of this study was to investigate the neural correlates of auditory processes with a fine spatio-temporal resolution. A simultaneous auditory evoked potentials (AEP) and functional magnetic resonance imaging (fMRI) technique (AEP-fMRI), together with an odd-ball paradigm, were used.





Material/Methods: Six healthy volunteers, aged 20–35 years, participated in an odd-ball simultaneous AEP-fMRI experiment. AEP in response to acoustic stimuli were used to model bioelectric intracerebral generators, and electrophysiological results were integrated with fMRI data.

Results: fMRI activation evoked by standard stimuli was found to occur mainly in the primary auditory cortex. Activity in these regions overlapped with intracerebral bioelectric sources (dipoles) of the N1 component. Dipoles of the N1/P2 complex in response to standard stimuli were also found in the auditory pathway between the thalamus and the auditory cortex. Deviant stimuli induced fMRI activity in the anterior cingulate gyrus, insula, and parietal lobes.

Conclusions: The present study showed that neural processes evoked by standard stimuli occur predominantly in subcortical and cortical structures of the auditory pathway. Deviants activate areas non-specific for auditory information processing.

MeSH Keywords: **auditory pathways • functional magnetic resonance imaging • central auditory system • auditory evoked potential**

Full-text PDF: <http://www.medscimonit.com/download/index/idArt/889712>

 4199  3  6  71

Background

An ability to select relevant auditory stimuli from our surroundings is an important aspect of human behavior. One commonly used experimental scheme for studying neural correlates of auditory processing is the odd-ball paradigm [1] in which a target acoustic stimulus (the deviant) is presented among frequent stimuli (the standard). The task is to respond (by pressing a button or counting silently) to the deviants and ignore the standard sounds [2]. An odd-ball paradigm is designed to involve both perception and processing of auditory information at higher levels [2,3].

The neural basis of auditory information processing has been investigated using various methods [4–8]. One of these techniques is auditory evoked potentials (AEP), in which cortical responses to acoustic stimuli are registered [9–12]. It is well documented [10] that the morphology of AEP elicited by a standard sound is different from the cortical response to a deviant. Accordingly, a standard stimulus (e.g. a pure tone) induces N1 and P2 components, which together constitute an N1/P2 complex. In response to deviants, N2 and P3 potentials are also observed, as well as N1 and P2 components [10,13]. Such differences in the morphology of AEP between deviant and standard stimuli result from the involvement of different structures in the processing of each stimulus type [14].

Certain components of AEP are considered to be markers of subsequent processes engaged during the processing of a stimulus (see [2,15] for a review). Early components of AEP such as N1, P2, or N1/P2 complex are considered exogenous and reflect neural processes associated mainly with sensory and physical properties of the stimuli, or detection of nonspecific physical or semantic changes in the hearing environment [16]. In contrast, later endogenous components are thought to be markers of cognitive processes allocated to the task [17]. According to recent theories, the P3 potential reflects attention and working memory-dependent processes of stimulus categorization [18–20], whereas the N2 component is related to the process of matching the incoming stimulus to its internally generated contextual pattern, which occurs before the categorization [21,22]. In summary, odd-ball paradigms permit electrophysiological techniques to be used in a way that can separate the different neural processes associated with standard and deviant stimuli.

AEP can provide information about the timing of cortical activations at different stages of auditory processing [13,17,18,22]. AEP allow insight into rapid neural processes because the technique has high temporal resolution (in the range of milliseconds) due to the way in which the electrical field changes are measured [13]. During recording of AEP, rapid changes in the electrical field, induced by neural activity, propagate immediately from the involved brain area to the surface of the head.

Therefore, in an odd-ball paradigm the processing underlying each type of stimulus (standard or deviant) is immediately reflected in the AEP [13,17].

Although EEG methods, including AEP, have high temporal resolution, their spatial resolution is limited to a few centimeters [23]. This rather poor resolution comes from distortion of the electrical field while conducting through the skull and other brain tissues. So while AEP reflect the bioelectrical activity of particular brain structures, they are widely distributed on the surface of the head [24]. Consequently, EEG techniques cannot provide precise information on the location of particular stages of auditory processing.

To improve EEG spatial resolution it is necessary to sample the topographical distribution of particular AEP components at a sufficient density. For this purpose, a large number of electrodes – 32, 64, 128, or even 256 channels – have been used [25,26], enabling precise location of AEP bioelectrical sources. However, existence of an inverse problem makes the determination of AEP generators difficult because a given surface map may have been produced by many possible source distributions. In other words, the inverse problem has no unique solution.

Intracerebral sources of particular AEP components can in theory be determined using various algorithms such as equivalent current dipoles (ECDs) or distributed source models [27,28]. A major limitation of the ECD technique is the requirement to make assumptions about the neural sources. ECDs usually assume that the underlying neuronal sources are focal. Such a supposition requires a thorough knowledge of neuroanatomy and neurophysiology, and it is only reasonable for motor or sensory processes that have a well-defined representation in the brain. However, for widely distributed cognitive processes, source modeling becomes very complicated [13].

Distributed source models (e.g. LORETA and sLORETA) divide the source space into a grid containing many dipoles. The inverse problem is to obtain the dipole moments for each grid node. As the number of unknown dipole moments is much greater than the number of electrodes, the inverse solution is highly underdetermined. In this technique, assumptions about the modeled EEG sources are not necessary [28,29], but the resulting distributions can be difficult to interpret because they only generate a blurred image of the neuronal source distribution. Neural sources modeling is constantly being developed to provide more precise locations of the EEG generators. However, all these techniques are very sensitive to signal distortion, and when the signal-to-noise ratio is low, source modeling is susceptible to errors [30].

In view of the limitations of EEG methods in determining the source of brain activity, functional magnetic resonance imaging

(fMRI) has been used to study neural processes evoked by standard and deviant acoustic stimuli (event-related fMRI) [31–36]. This technique is based on blood-oxygen level-dependent (BOLD) contrast, discovered by Ogawa [37], and is used to map neural activity in the brain with a high spatial resolution (a few millimeters). The technique relies on cerebral blood flow and neuronal activation being coupled. When a brain area is engaged in a task, blood flow to that region increases. Therefore, an fMRI study using an auditory odd-ball paradigm allows recording the BOLD signal from areas activated during the processing of standard and deviant stimuli. However, a limitation of the fMRI technique is its low temporal resolution. The resulting fMRI images show all brain structures activated during a whole cycle of hemodynamic response, which takes several seconds [37]. During this time many different neural processes may occur and all of them are reflected in the fMRI images.

Taking all the above facts into consideration, investigation of rapid and complex neural processes is a methodological challenge. One approach to solving this problem is to combine 2 techniques, one with high spatial resolution and the other with high temporal resolution. For example, AEP recording can be performed simultaneously with MEG or PET [38,39], but most studies use a combination of AEP and fMRI methods. Combination of these techniques creates a powerful tool for studying processing at different levels of the auditory pathway [40,41].

During the past several years, high spatio-temporal resolution methods have been used to investigate the neural processes engaged in an auditory odd-ball task. However, most of these studies focus on the brain activities related to deviants [34,36,42,43]. Only a few authors have attempted to describe processes and structures involved in both deviant and standard stimuli analysis [44,45], which appears to be a promising approach to investigate the processes occurring at different stages of the auditory system.

Here, we present the preliminary results of studies on neural correlates of stimulus processing in the auditory odd-ball paradigm. Simultaneous AEP-fMRI technique was applied to measure deviant and standard induced brain activity, with good spatial and temporal resolution. Both AEP-fMRI method and an experimental procedure may be used to investigate auditory information processing at different levels of the central nervous system in clinical samples.

Material and Methods

The AEP-fMRI study was conducted at the Bioimaging Research Center of the Institute of Physiology and Pathology of Hearing in Warsaw, Poland.

Subjects

Six young adults (5 male and 1 female), aged 22 to 35 years, participated in the study. All subjects had normal hearing levels in both ears (below 20 dB HL for 125, 250, 500, 750, 1000, 1500, 2000, 4000, and 8000 Hz), relatively good health, were right-handed (*Edinburgh Handedness Inventory* [46]) and reported no history of neuropsychiatric disorders.

General exclusion criteria for AEP-fMRI study are ferromagnetic objects in the body and claustrophobia. During simultaneous registration of AEP and fMRI, signal subjects are asked to lie down in the same position in a limited space for about half an hour. For this reason, the AEP-fMRI procedure is not recommended for pregnant women, very young children, persons with hyperactivity, or those more prone to fatigue (e.g. elderly people and post-stroke patients).

Each subject provided written informed consent prior to the study. The study was performed in accordance with the Declaration of Helsinki and was approved by the local ethics committee.

Subject preparation and data acquisition procedure

The main AEP-fMRI study was preceded by certain preparatory activities such as the attachment of electrodes (mounted in a special cap) to the subject's head, application of a gel to the electrodes to improve the conduction of electrical impulses, measurement of impedance of the electrodes, and, finally, placing the subject in an MRI scanner. The preparation procedure took about 30 min.

The AEP-fMRI study consisted of 2 parts: acquisition of anatomical images of the whole brain and simultaneous registration of AEP and fMRI signal in response to presented auditory stimuli. The entire AEP-fMRI study (including preparation procedure) lasted about 30 min. After completing the AEP-fMRI study, each subject had a short (15–20 min) time to rest. Then, AEP registration was performed outside an MR scanner room which took approximately 10 min. The entire procedure took 1.5 h.

Experimental paradigm

A modified auditory odd-ball paradigm was used to acquire AEP inside an MRI scanner (Figure 1). Pure sinusoidal 100-ms tones of different frequency (1 and 2 kHz) were delivered binaurally via electrostatic headphones at 80 dBA hearing level. The stimuli were presented in 2 alternating 30-s blocks: 1) a standard and 2) an odd-ball block. There were 10 repetitions of each block. The standard block consisted of ten 1-kHz tones, whereas the odd-ball block consisted of three 2-kHz tones (deviants) and seven 1-kHz tones (standards) presented in pseudo-random order.

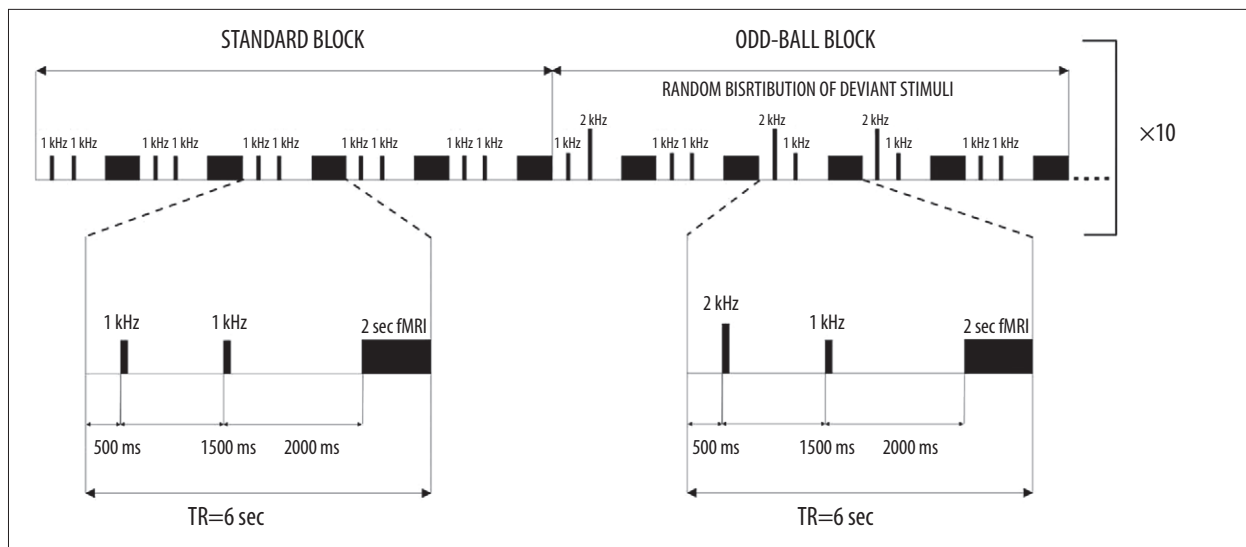


Figure 1. The paradigm sequence. The upper part of the figure shows an example of two 30-second stimulation blocks (a standard and an odd-ball block) randomly selected from 20 blocks administered during a whole experiment. The lower part of the figure shows the detailed arrangement of individual stimuli within each block. The time interval between successive fMRI scans was 6 seconds (TR – repetition time).

During the standard block, subjects were asked to listen attentively to the applied stimuli. The odd-ball task was to silently count the deviants and ignore the more frequently presented standards. During a whole run on a single subject, 30 AEP to deviants and 170 responses to standard stimuli were registered.

fMRI data were collected according to the SPARSE acquisition schema, which allows stimuli to be presented in the absence of scanner noise [47]. Figure 1 shows the stimulus scheme, in which every 6-s interval within the standard or oddball block contained 2 tones, 2 s of silence, and then a whole brain scan occupying another 2 s.

AEP acquired in the magnet were compared with the electrophysiological responses obtained outside the MRI scanner. The paradigm used outside the scanner was virtually the same as that applied during the combined AEP-fMRI study, the only difference being the lack of scanning periods. The studies inside and outside the scanner were performed in a single session and were counterbalanced across subjects.

EEG data acquisition and signal preparation

AEP were registered from 62 unipolar electrodes placed on the subject's head according to the 10/10 International Standard System [48] using a MagLink (Neuroscan) EEG recording system from Compumedics, which is designed to work in strong magnetic fields. Two pairs of bipolar electrodes were used to monitor vertical eye movements (VEOG) and the electrocardiogram (ECG). The ground electrode was placed between FCz and Fz, and the reference electrode for all unipolar electrodes was

located between CPz and Cz. The impedance of each channel was kept below 10 k Ω .

The electrophysiological data acquired during the simultaneous AEP-fMRI recordings (outside and inside the MRI scanner) were analyzed according to the following procedure. Large (thousands of μ V) gradient artifacts (GAs) were first removed from the EEG signal (GAs are induced in EEG signals by magnetic field changes in the gradient coils of the MRI scanner [49]). GAs did not interfere directly with AEP recorded during the silent intervals; however, their removal helps visualize the EEG signal and thereby improves signal processing. A high (10 kHz) sampling rate was used to remove GAs from the EEG data by subtraction of the averaged template. A corresponding template for each gradient coil activation was based on 17 artifacts surrounding the currently processed 2-s block.

Balistocardiogram (BCG) artifacts were also removed from the EEG signal. BCG artifacts are generated by heart beats, which change the position of EEG electrodes and wires on the subject's head and body and induce spurious voltages [49]. A modified procedure [50,51] was performed to reduce BCG artifacts. Each well-defined QRS complex was manually marked at maximum amplitude of the R peak and then used to create a separate average BCG artifact template for each channel. These templates were used to calculate a singular value decomposition (SVD) matrix, which formed the basis of BCG component reduction.

Artifacts induced by eye movements were also removed using the same procedure as BCG artifact reduction. After the removal

of artifacts, standard AEP analysis was conducted. The recording window consisted of a 100-ms pre-stimulus period and a 750-ms post-stimulus time. Baseline correction and band-pass filtering (1–30 Hz, 12 dB/octave, no phase shift) of each epoch was performed and the signal was averaged.

Study design and fMRI data analysis

The fMRI study was performed using a high-field (3T) Siemens Magnetom Trio Tim MRI scanner. The scanning function had the following parameters: T2 single-shot echo-planar imaging, EPI sequence, voxel size =3×3×4 mm, 32 axial slices, repetition time (TR) =6000 ms, echo time (TE) =30 ms, acquisition time (TA) =10 min.

For structural imaging, a T1 inversion recovery sequence with the following parameters was used: voxel size =0.9×0.9×0.9 mm, 208 sagittal slices, repetition time (TR)=1900 ms, echo time (TE)=2.21 ms, inversion time (TI)=900 ms, and acquisition time (TA)=5 min.

fMRI data obtained during simultaneous fMRI-EEG signal recording was analyzed in the SPM8 toolbox for MATLAB. Preprocessing of the brain images included movement correction (first volume was used as the reference image), co-registration with the subject's structural brain image, and smoothing using a Gaussian spatial filter with voxel FWHM of 6 mm. A general linear model (GLM) and a high-pass filter with a period of 128 s were used to analyze BOLD signal changes. Additionally, hemodynamic response function (HRF) modeling was applied.

For each subject, the standard vs. deviant and deviant vs. standard contrasts were calculated (the first-level analysis). Then, a 1-sample *t* test (*p*-value threshold ≤0.01) was applied for group data analysis (the second-level analysis).

3D spatial current distribution modeling and intracerebral AEP source analysis

A brain-mapping technique was used to model the spatial distribution of AEP voltages [52]. Modeling was done on the bioelectric responses recorded from all electrodes during sessions outside and inside the MRI scanner. Three-dimensional distribution maps of particular AEP components were calculated and projected onto virtual and real head models (the latter created from MRI images of the subjects).

The 3D voltage distribution maps and AEP recorded from all 62 electrodes during the combined AEP-fMRI study were used to localize the intracerebral sources (dipoles) of evoked responses. Two different methods – rotating and moving dipoles – were used to calculate AEP generators [30]. Dipoles

of subsequent components visible in the AEP to standard and deviant stimuli were modeled separately. To specify the AEP generators, time intervals during which the mean global field power (MGFP) of the modeled components reached maximum values were used. To fix the number of sources to be modeled, independent component analysis (ICA) was applied to signals in each of the predefined time ranges. The number of ICA components that explained the majority of the AEP variance was assumed to be the number of intracerebral sources for each modeled component.

Calculation of spatial distribution and intracerebral sources (generators) of AEP was done using Curry 6.0 software (Compumedics Neuroscan, Charlotte, NC).

Combining AEP and fMRI results

The same Curry 6.0 software was also used to combine the electrophysiological and fMRI data. The dipoles of particular AEP components uncovered by the intracerebral source analysis were combined with fMRI hemodynamic activation data.

Results

The results of AEP and fMRI analyses were integrated to provide data with high spatial and temporal resolution.

Brain response to deviant stimuli

Figure 2 shows the average AEP to deviants averaged across all subjects. It presents electrode responses recorded during simultaneous AEP-fMRI (grey lines) compared to cortical responses obtained outside the MRI scanner (black lines). Outside the scanner, N1, P2, and P3 (P300) components could be observed in all study subjects. However, inside the magnet these components had smaller amplitudes and, as Figure 2 shows, could be clearly distinguished, predominantly at central electrodes. Mean amplitudes and latencies of individual response components for deviant tones measured at C3 electrode are shown in Table 1.

Deviant stimuli activated bilateral insula and inferior parietal lobule as well as left anterior cingulate gyrus (Table 2).

Brain response to standard stimuli

AEP to standard stimuli inside and outside the MRI scanner had a similar morphology at all electrodes (Figure 3). Specifically, N1 and P2 components were observed in both conditions. Latencies of the components were comparable, but the amplitudes were higher outside the magnet than inside (Table 3). Moreover, distribution of N1 and P2 amplitudes, acquired

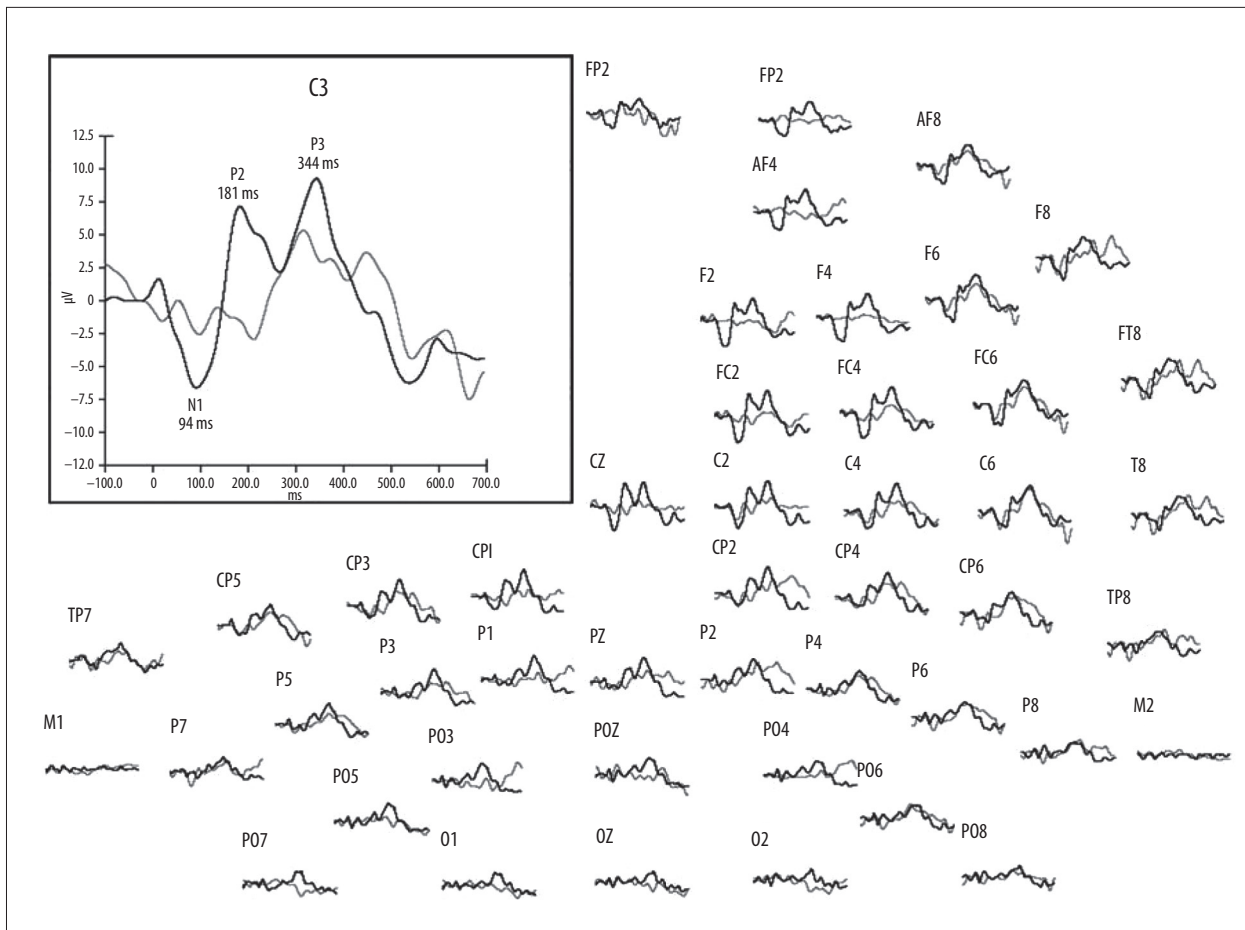


Figure 2. Auditory evoked potentials to deviant stimuli (2000 Hz) recorded from 64 electrodes and averaged across all subjects. Grey lines show AEP recorded during the AEP-fMRI study inside the MRI scanner, with black lines showing AEP registered outside the scanner. The enlarged window shows detail of the N1, P2, and P3 components recorded at the C3 electrode.

Table 1. Mean amplitudes and latencies of AEP to 2000 Hz deviant stimuli recorded at the C3 electrode during measurements outside the MRI scanner.

Auditory evoked potential component	Mean value of AEP parameter obtained outside MRI scanner	
	Amplitude	Latency
N1	-4.5 μ V (\pm 1.5)	109.8 ms (\pm 5.6)
P2	5.5 μ V (\pm 1.2)	186.5 ms (\pm 5.0)
P3	6.5 μ V (\pm 2.8)	332.4 ms (\pm 20.4)

during the simultaneous AEP-fMRI study, matched the topography of the corresponding components recorded outside the MRI scanner. Topographies of the N1 and P2 amplitudes registered inside and outside the MRI scanner were similar to those observed outside the MRI scanner (Figure 4 shows the distribution of amplitudes laid out on the virtual head model).

The AEP of individual subjects recorded inside the MRI scanner in response to standard stimuli were used to model the dipoles (intracerebral sources of bioelectric activity) of the N1 component. The procedure began from an AEP amplitude distribution plotted on the surface of a real head model created from an MRI image of the subject. Figure 5B presents an example of an N1 component amplitude distribution mapped onto a model of a subject's head. The sources of the N1 component were calculated using the method of rotating dipoles [30]. This technique reduces the location of intracerebral sources to fixed points inside the brain space, but allows for changes in orientation and strength of the dipoles. Based on the results of ICA analysis, 2 symmetrical sources of N1 were modeled. The dipoles were calculated within the latency range in which the MGFP of the N1 component reaches its maximal value. Figure 5A shows the results of such analysis, revealing 2 separate N1 generators located near the primary auditory cortex.

The intracerebral sources of the N1/P2 complex evoked by standard stimuli were also modeled using the moving dipoles

Table 2. Results of deviant-to-standard and standard-to-deviant fMRI contrast analysis obtained during simultaneous AEP-fMRI recording. The columns show brain regions, coordinates of activated voxels having maximum *t* statistics in Talairach's space, number of activated voxels, and *t* values ($p \leq 0.01$ without correction of multiple comparisons).

Brain region	fMRI	Number of activated voxels	Contrast
	X, Y, Z (Talairach)		
Deviant to standard t			
Insula (left hemisphere)	40, 12, -4	441	4.98
Insula (right hemisphere)	-42, 10, 2	228	4.34
Anterior cingulate gyrus (left hemisphere)	2, 18, 46	409	7.80
Inferior parietal lobule (left hemisphere)	32, -56, 42	607	6.28
Inferior parietal lobule (right hemisphere)	-36, -68, 48	993	8.24
Standard to deviant t			
Primary auditory cortex (left hemisphere)	50, -2, 0	979	5.72
Primary auditory cortex (right hemisphere)	-48, -26, 8	819	5.12

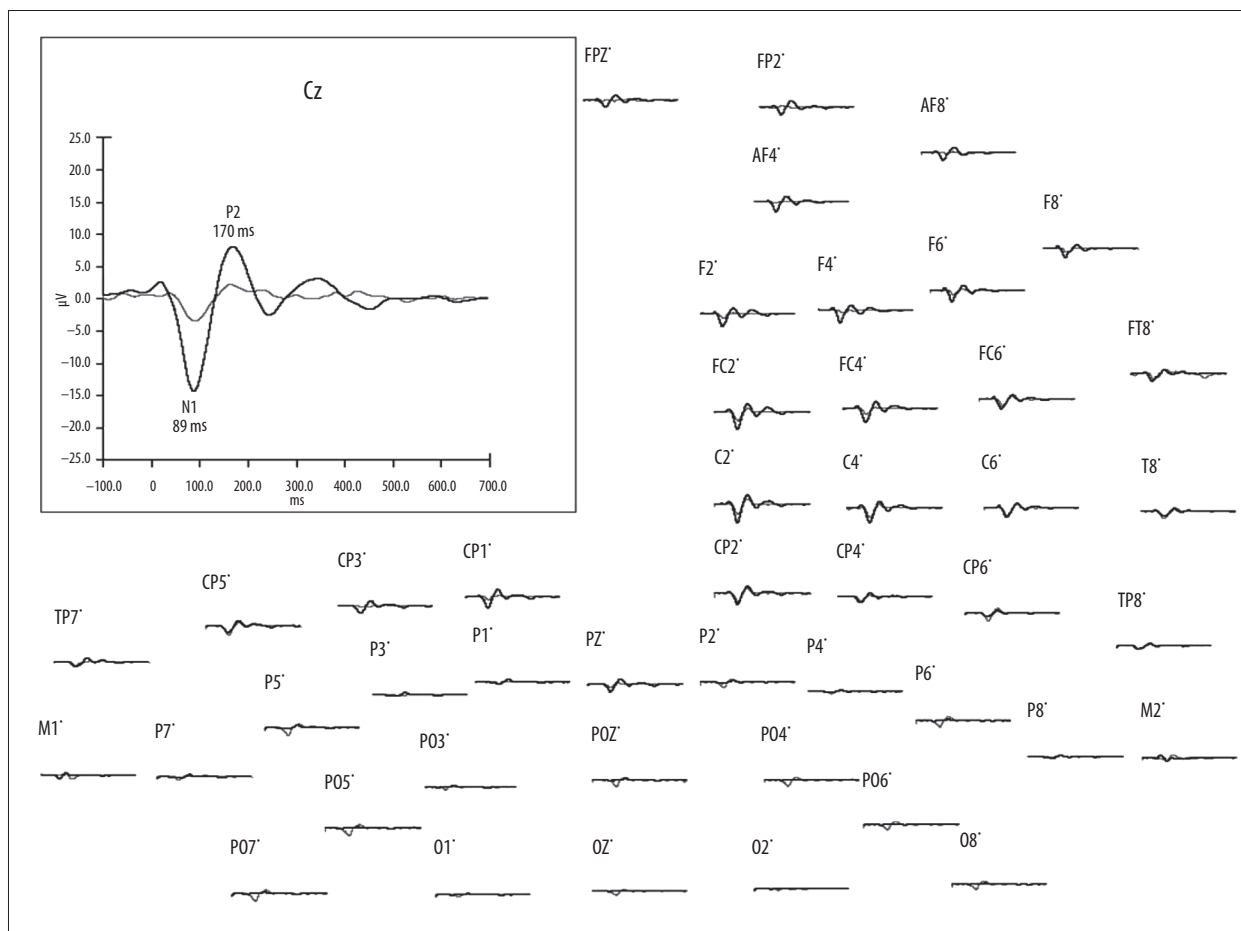


Figure 3. Auditory evoked potentials to standard stimuli (1000 Hz) recorded from 64 electrodes and averaged across all subjects. Grey lines show AEP recorded during the AEP-fMRI studies performed inside the MRI scanner, with black lines showing AEP registered outside the scanner. The enlarged window shows detail of the N1 and P2 components recorded from the Cz electrode.

Table 3. Mean amplitudes and latencies of AEP generated in response to 1000 Hz standard stimuli and recorded at the Cz electrode while outside the MRI scanner (left column) and during simultaneous AEP-fMRI (right).

	Outside MRI scanner room	Inside MRI scanner room
Mean amplitude of AEP component		
N1	-13.8 μ V (\pm 1.2)	-7.3 μ V (\pm 2.1)
P2	6.07 μ V (\pm 1.0)	4.07 μ V (\pm 1.5)
Mean latency of AEP component		
N1	85.90 ms (\pm 5.1)	92.0 ms (\pm 6.3)
P2	166.7 ms (\pm 4.7)	167.2 ms (\pm 5.1)

technique. All parameters of the dipoles, including locations, were allowed to vary [30]. The moving dipoles method confirmed the results of the rotating dipoles technique (ie, 2 symmetrical dipoles of the N1/P2 complex were modeled). The N1/P2 generators (calculated at times within the N1/P2 latency of 50–120 ms) were located in brain regions where subsequent stages of information processing take place. These regions are part of the auditory pathway between the thalamus and auditory cortex (Figure 6A–6C). It is noteworthy that fMRI data also indicates activation of the primary auditory cortex in response to standard stimuli (Table 2).

To obtain data displaying both good temporal and spatial resolution, results of the moving dipole analysis of the N1/P2 complex were integrated with the fMRI outcomes. The N1/P2 generators were superimposed on the MRI images and then compared with the fMRI activations in response to the same

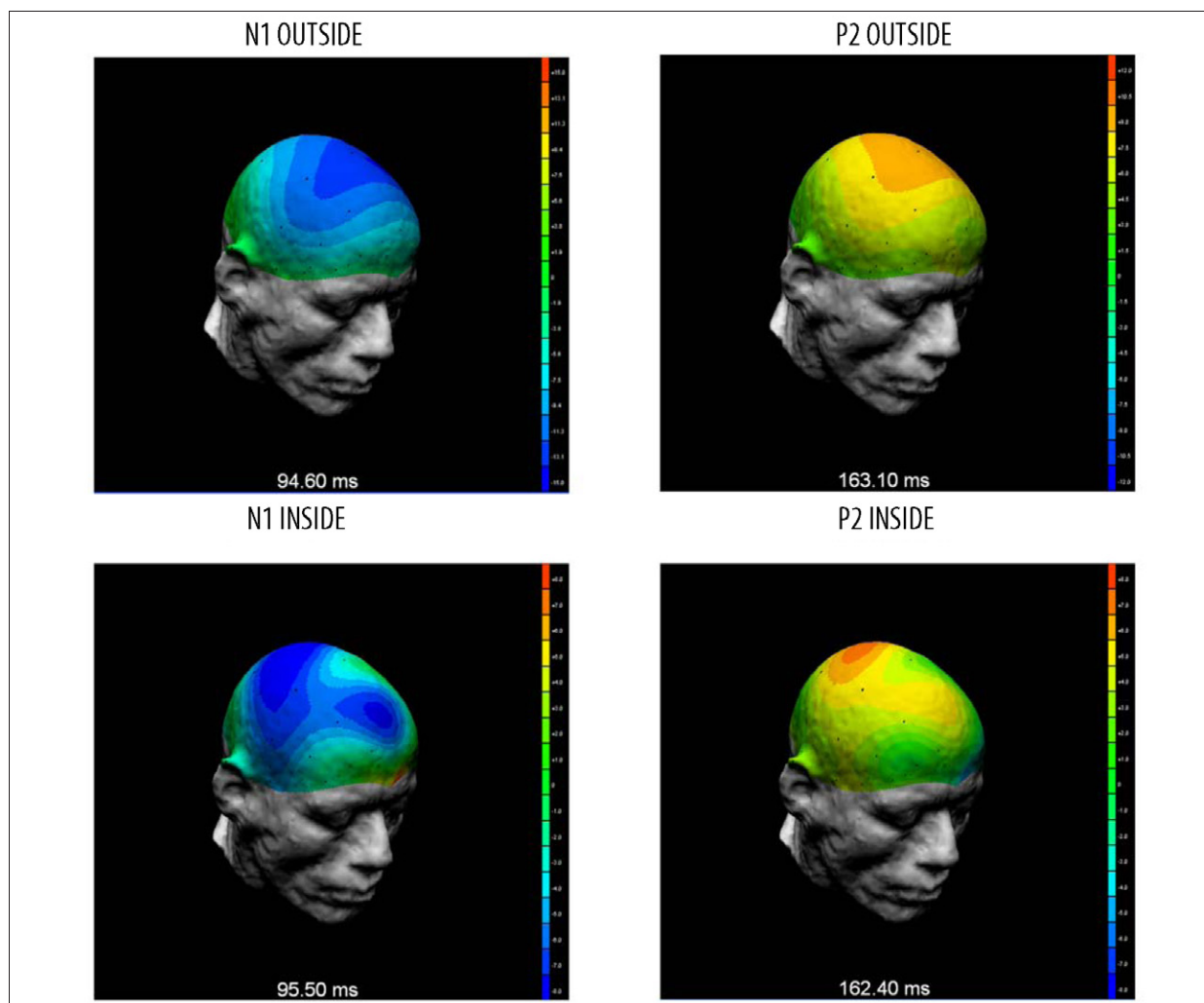


Figure 4. Scalp distributions of N1 and P2 amplitudes superimposed on a virtual head and calculated from signals recorded from all electrodes both outside (top) and inside (bottom) the MRI scanner. Images show the distributions of average AEP to standard stimuli calculated from data of all (6) subjects.

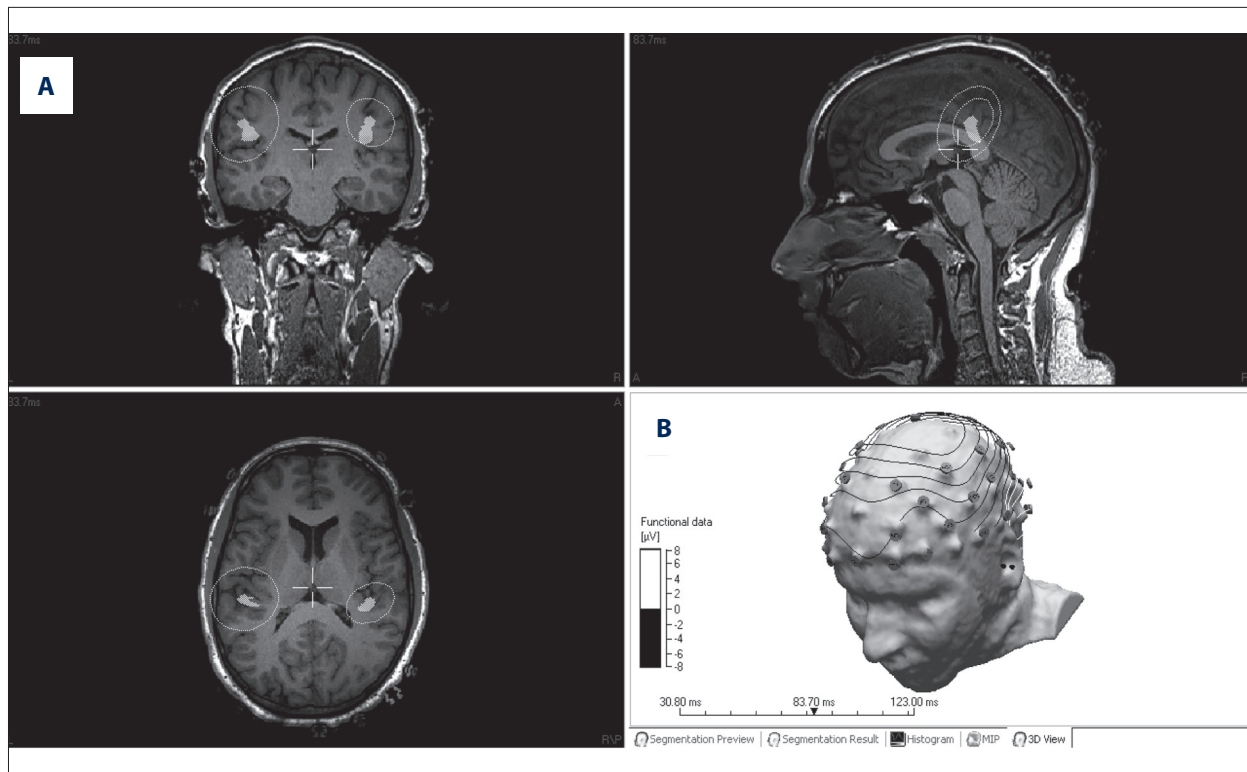


Figure 5. (A) Intracerebral sources (dipoles) of the N1 component in response to standard stimuli (1000 Hz), modeled for the latency range during which the MGPF component reached its maximum and superimposed on three cross-sections of a structural MRI brain image for a single subject. (B) Spatial distribution of N1 amplitude on the subject's head, calculated on the basis of AEP acquired from all 64 electrodes during simultaneous AEP-fMRI study and from which the N1 dipoles were calculated.

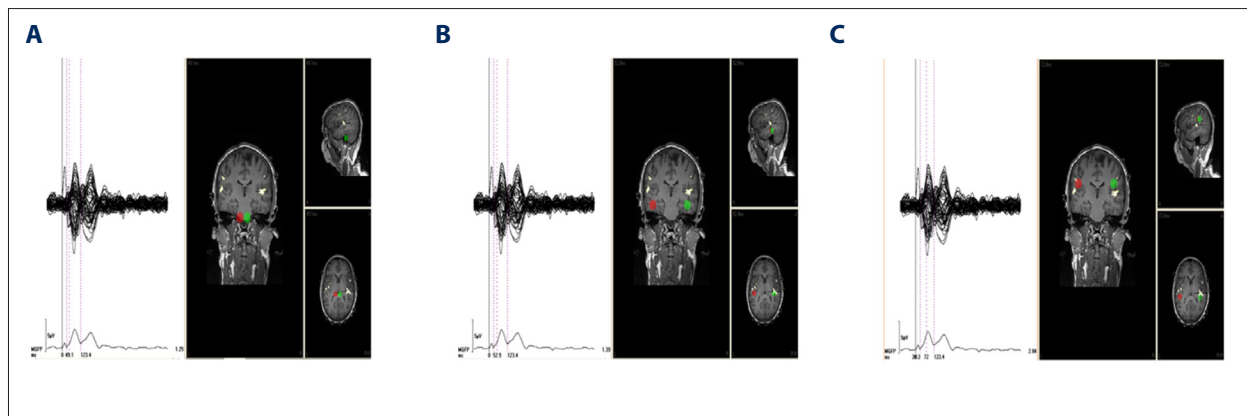


Figure 6. AEP (left) and hemodynamic responses (right) to 1000 Hz standard stimuli acquired during simultaneous AEP-fMRI. The butterfly plots at left show AEP from 64 electrodes, with the average magnitude shown below. Dipole sources of the N1/P2 complex (red and green) were calculated at (A) 50 ms, (B) 53 ms, and (C) 72 ms after stimulus presentation and superimposed (color) on three cross-sections of a single subject's MRI structural image. fMRI activations related to standard stimuli are depicted in yellow color.

stimuli. In most subjects (5 out of 6) the N1/P2 dipoles, modeled at a time when each component's amplitude was at a maximum, appeared at locations close to the primary auditory cortex (Figure 6C). Similar as previously, fMRI data showed the same brain regions to be active (Figure 6A–6C).

Discussion

The aim of the present AEP-fMRI study was to define, both in time and space, the neural processes and areas of the brain involved in processing standard and deviant stimuli. We used

an auditory odd-ball paradigm, and AEP evoked by 1000 Hz (standard) and 2000 Hz (deviant) tones were recorded simultaneously with hemodynamic (fMRI) responses triggered by these 2 stimulus types.

We obtained bioelectrical (AEP) responses to standard and deviant stimuli, and the morphology of individual AEP components and their parameters (amplitude and latency) to both these stimulus types were compared to AEP evoked by the same stimuli outside the MRI scanner (Figures 2, 3). AEP components induced inside the scanner had smaller amplitudes compared to those outside the scanner room. Others have also found similar reductions [53–55], and one possibility is that this might be due to constant activation of the auditory cortex from noise generated by the MRI gradient coils (approximately 99 dB SPL) [53].

Our AEP-fMRI study showed that electroencephalographic responses to standard stimuli were localized to the primary auditory cortex (Figures 5A, 6C and Table 2). These results are in accordance with reports on neural processes evoked by standard stimuli using both fMRI [56,57] and simultaneous AEP-fMRI [44,45,51]. In our studies, the primary auditory cortex was stimulated by frequent acoustic stimuli presented in an odd-ball paradigm. In contrast to standard stimuli, deviants activated structures that are not part of the central auditory system (ie, the inferior parietal lobule, anterior cingulate gyrus, and insula (Table 2). Similar brain activations have been found in previous studies using experimental paradigms that involved cognitive or emotional processes [58,59]. Such studies used AEP, fMRI, and either simultaneous AEP-fMRI or VEP-fMRI to determine P3 generators [34,60–62]. Previous work has also indicated that the inferior parietal lobule is engaged in tasks requiring decision making [63] and has been considered to play important role in visuo-motor integration and spatial perception [64], emotion recognition [65], language [66], and mathematical reasoning [67].

In response to standard stimuli, our study was able to locate the intracerebral bioelectrical generators of individual components of the AEP. We used the moving and rotating dipoles techniques, and both methods provide results corresponded with the fMRI findings. Obtained locations of the intracerebral bioelectrical generators were also congruent with the results reported by other authors [45,51]. However, the deviant tones work was a different matter – when we attempted to determine the generators of the N1, P2 or N1/P2 complex, and P3 using such stimuli, and combine them with fMRI and MRI data, locations of the modeled dipoles did not completely overlap with fMRI activations. This effect might result from a low signal-to-noise ratio in AEP in responses to deviants. A minimal signal-to-noise ratio (SNR) in the EEG signals used for modeling the intracerebral bioelectrical generator to achieve reliable

results should be <4 [68,69]. In our study, SNR for AEP to deviants was below this value, so in this case we decided to not interpret the results of modeling of AEP generators. Low SNR in EEG signal recorded in the magnet in responses to deviants might be caused by specific experimental conditions during simultaneous AEP and fMRI data registration; a high magnetic field induces specific artifacts in EEG signal leads to decreasing SNR ratio [70]. Moreover, the relatively small number of deviants ($n=30$) applied in our odd-ball paradigm most likely contributed to a low SNR value. Presentation of more deviant stimuli would, however, significantly extend the testing time inside an MRI scanner, leading to subject fatigue and decreasing motivation to perform the auditory task [71]. A number of infrequent stimuli used in our odd-ball paradigm theoretically should enable modeling AEP generators, but, unfortunately, it turned out to be insufficient. Therefore, we suggest an increased number of deviants and perhaps some modifications of an experimental protocol in an AEP-fMRI procedure. Such improvements would allow for more pronounced brain (bioelectrical and hemodynamic) responses and a relatively short testing time. In this case, a paradigm could be suitable not only for young adults but also for children, elderly people, and clinical trials.

Conclusions

The presented AEP-fMRI odd-ball paradigm allows examination of the neural processes related to analysis of deviant and standard stimuli, with high spatio-temporal resolution. In responses to deviant stimuli, we found activations in the cortical regions not directly involved in the central auditory processes, whereas both low (subcortical) and high (cortical) levels of the auditory system were engaged in the standards processing.

A method of simultaneous AEP and fMRI signal registrations combines fMRI's ability to precisely locate the blood dynamics in the whole brain with the electrophysiological ability to characterize rapid neural processes and to reveal pathological patterns. Therefore, our AEP-fMRI study might provide clinically useful information about the functioning of the central auditory system.

Because of the prolonged testing time inside an MRI scanner and the complexity of the procedure, we recommended the presented odd-ball paradigm for adult and relatively cooperative patients. However, this protocol, after small modifications, might also be adapted to investigate central auditory information processing in clinical trials.

Acknowledgments

The authors are grateful to Andrew Bell for valuable comments on the paper. We also would like to thank Wiktor Wiesław

Jedrzejczak, Agnieszka Pluta, and Kinga Wolujewicz for reviewing this article and making helpful suggestions.

References:

1. Squires NK, Squires KC, Hillyard SA. Two varieties of long-latency positive waves evoked by unpredictable auditory stimuli in man. *Electroencephalogr Clin Neurophysiol*, 1975; 38: 387–401
2. Eichele T. *Electrophysiological and Hemodynamic Correlates of Expectancy in Target Processing*. 2007. PhD Thesis. The University of Bergen. Available from: <http://hdl.handle.net/1956/2509>
3. Mangalathu Arumana J: Integration of EEG-fMRI in an auditory oddball paradigm using joint independent component analysis. 2012. Available from: http://epublications.marquette.edu/cgi/viewcontent.cgi?article=1212&context=dissertations_mu
4. Lalaki P, Hatzopoulos S, Lorito G et al: A connection between the Efferent Auditory System and Noise-Induced Tinnitus Generation. Reduced contralateral suppression of TEOAEs in patients with noise-induced tinnitus. *Med Sci Monit*, 2011; 17(7): MT56–62
5. Bembich S, Demarini S, Clarici A et al: Non-invasive assessment of hemispheric language dominance by optical topography during a brief passive listening test: A pilot study. *Med Sci Monit*, 2011; 17(12): CR692–97
6. Allendorfer J, Kissela B, Holland S, Szaflarski J: Different patterns of language activation in post-stroke aphasia are detected by overt and covert versions of the verb generation fMRI task. *Med Sci Monit*, 2012; 18(3): CR135–47
7. Raumane D, Kise L, Logina I: Auditory Behavioural and Electrophysiological Responses in Adults: Evaluating Central Auditory Processing. *Journal of Hearing Science*, 2013; 3(1): 9–17
8. Skarzyński PH, Wolak T, Skarzyński H et al: Application of the functional Magnetic Resonance Imaging (fMRI) for the Assessment of the Primary Auditory Cortex Function in Partial Deafness Patients – A preliminary study. *Journal of International Advanced Otology*, 2013; 9(2): 153–60
9. Segalowitz SJ, Barnes KL: The reliability of ERP components in the auditory odd-ball paradigm. *Psychophysiology*, 1993; 30: 451–59
10. McPherson DL, Ballachanda BB, Kaf W: Middle and long latency auditory evoked potentials. *Audiology Diagnosis* 2nd ed. New York: Thieme, 2007; 443–78
11. Hatzopoulos S, Petrucci J, Šliwa L et al: Hearing threshold prediction with Auditory Steady State Responses and estimation of correction functions to compensate for differences with behavioral data, in adult subjects. Part 1: Audaera and CHARTER EP devices. *Med Sci Monit*, 2012; 18(7): MT47–53
12. Trzaskowski B, Jedrzejczak WW, Pilka E et al: Automatic removal of sonomotor waves from auditory brainstem responses. *Comput Biol Med*, 2013; 43(5): 524–32
13. Luck SJ: *An introduction to the event-related potential technique (cognitive neuroscience)*. 1st ed. Cambridge: The MIT Press, 2005
14. Wunderlich JL, Cone-Wesson BK: Maturation of CAEP in infants and children: a review. *Hear Res*, 2006; 212: 212–23
15. Kotchoubey B: Event-related potentials, cognition, and behavior: a biological approach. *Neurosci Biobehav Rev*, 2006; 30: 42–65
16. Näätänen R, Picton T: The N1 wave of the human electric and magnetic response to sound: a review and an analysis of the component structure. *Psychophysiology*, 1987; 24: 375–425
17. Fabiani M, Gratton G, Coles MGH: Event related brain potentials: methods, theory and applications. In: Cacioppo J, Tassinary L, Berntson G (eds.), *Handbook of Psychophysiology*. 3rd ed. New York: Cambridge University Press, 2007; 53–84
18. Polich J: Theoretical overview of P3a and P3b. In: Polich J (ed.), *Detection of Change: Event-Related Potential and fMRI findings*. 1st ed. Massachusetts: Kluwer Academic Publishers, 2003; 83–98
19. Polich J: Updating P300: an integrative theory of P3a and P3b. *Clin Neurophysiol Off J Int Fed Clin Neurophysiol*, 2007; 118: 2128–48
20. Pačalska M, Kropotov ID, Mańko G et al: Evaluation of a neurotherapy program for a child with ADHD with Benign Partial Epilepsy with Rolandic Spikes (BPERS) using event-related potentials. *Med Sci Monit*, 2012; 18(11): CS94–104
21. Näätänen R, Simpson M, Loveless NE: Stimulus deviance and evoked potentials. *Biol Psychol*, 1982; 14: 53–98
22. Näätänen R: *Attention and brain function*. 1st ed. Hillsdale (NJ): Lawrence Erlbaum, 1992
23. Freeman WJ, Holmes MD, Burke BC, Vanhatalo S: Spatial spectra of scalp EEG and EMG from awake humans. *Clin Neurophysiol*, 2003; 114(6): 1053–68
24. Nunez PL: *Electric fields of the brain: the neurophysics of EEG*. 2nd ed. Oxford: Oxford University Press, 2006
25. Michel CM, Lantz G, Spinelli L et al: 128-channel EEG source imaging in epilepsy: clinical yield and localization precision. *J Clin Neurophysiol*, 2004; 21: 71–83
26. Slotnick SD: High Density Event-related Potential Data Acquisition in Cognitive Neuroscience. *J Vis Exp*, 2010; 38: 1945
27. Scherg M: Fundamentals of dipole source potential analysis. *Audit Evoked Magn Fields Electr Potentials Adv Audiol*, 1990; 6: 40–69
28. Pascual-Marqui RD, Michel CM, Lehmann D: Low resolution electromagnetic tomography: a new method for localizing electrical activity in the brain. *Int J Psychophysiol*, 1994; 18: 49–65
29. Pascual-Marqui RD: Standardized low-resolution brain electromagnetic tomography (sLORETA): technical details. *Methods Find Exp Clin Pharmacol*, 2002; 24: 5–12
30. Pizzagalli DA: Electroencephalography and high-density electrophysiological source localization. In: Cacioppo J, Tassinary L, Berntson G (eds.), *Handbook of Psychophysiology*. 3rd ed. New York: Cambridge University Press, 2007; 56–84
31. Casey BJ, Forman SD, Franzen P et al: Sensitivity of prefrontal cortex to changes in target probability: a functional MRI study. *Hum Brain Mapp*, 2001; 13: 26–33
32. Clark VP, Fannon S, Lai S et al: Responses to rare visual target and distractor stimuli using event-related fMRI. *J Neurophysiol*, 2000; 83: 3133–39
33. Kirino E, Belger A, Goldman-Rakic P, McCarthy G: Prefrontal activation evoked by infrequent target and novel stimuli in a visual target detection task: an event-related functional magnetic resonance imaging study. *J Neurosci*, 2000; 20: 6612–18
34. Linden DE, Prvulovic D, Formisano E et al: The functional neuroanatomy of target detection: an fMRI study of visual and auditory odd-ball tasks. *Cereb Cortex*, 1999; 9: 815–23
35. McCarthy G, Luby M, Gore J, Goldman-Rakic P: Infrequent events transiently activate human prefrontal and parietal cortex as measured by functional MRI. *J Neurophysiol*, 1997; 77: 1630–34
36. Stevens AA, Skudlarski P, Gatenby JC, Gore JC: Event-related fMRI of auditory and visual odd-ball tasks. *Magn Reson Imaging*, 2000; 18: 495–502
37. Ogawa S, Lee T-M, Nayak AS, Glynn P: Oxygenation-sensitive contrast in magnetic resonance image of rodent brain at high magnetic fields. *Magn Reson Med*, 1990; 14: 68–78
38. Gamma A, Lehmann D, Frei E et al: Comparison of simultaneously recorded H215O]-PET and LORETA during cognitive and pharmacological activation. *Hum Brain Mapp*, 2004; 22: 83–96
39. Pantazis D, Simpson GV, Weber DL et al: A novel ANCOVA design for analysis of MEG data with application to a visual attention study. *NeuroImage*, 2009; 44: 164–74
40. Goebel R, Esposito F: The added value of EEG-fMRI in imaging neuroscience. In: Mulert C, Lemieux L *EEG-fMRI: Physiological Basis, Technique, and Applications*, 1st ed. Berlin Heidelberg: Springer, 2010; 97–112
41. Mulert C: What Can fMRI add to the ERP story? In: Mulert C, Lemieux L (eds.), *EEG-fMRI Berlin Heidelberg*: Springer, 2010; 83–95
42. Kiehl KA, Stevens MC, Laurens KR et al: An adaptive reflexive processing model of neurocognitive function: supporting evidence from a large scale (n=100) fMRI study of an auditory odd-ball task. *NeuroImage*, 2005; 25: 899–915

Declaration of interest

The authors report no conflicts of interest. The authors alone are responsible for the content and writing of the paper.

43. Friedman D, Goldman R, Stern Y, Brown TR: The brain's orienting response: an event-related functional magnetic resonance imaging investigation. *Hum Brain Mapp*, 2009; 30: 1144-54
44. Liebenthal E, Ellingson ML, Spanaki MV et al: Simultaneous ERP and fMRI of the auditory cortex in a passive odd-ball paradigm. *Neuroimage*, 2003; 19: 1395-404
45. Mulert C, Seifert C, Leicht G et al: Single-trial coupling of EEG and fMRI reveals the involvement of early anterior cingulate cortex activation in effortful decision making. *Neuroimage*, 2008; 42: 158-68
46. Oldfield RC: The assessment and analysis of handedness: the Edinburgh inventory. *Neuropsychologia*, 1971; 9: 97-113
47. Bagshaw AP, Benar CG: Scanning strategies for simultaneous EEG-fMRI recordings. *Simultaneous EEG fMRI Rec Anal Appl Rec Anal Appl*, 2010; 85
48. Chatrian GE, Lettich E, Nelson PL: Modified Nomenclature for the "10%" Electrode System1. *J Clin Neurophysiol*, 1988; 5: 183-86
49. Herrmann CS, Debener S: Simultaneous recording of EEG and BOLD responses: a historical perspective. *Int J Psychophysiol*, 2008; 67: 161-68
50. Ille N, Berg P, Scherg M: Artifact correction of the ongoing EEG using spatial filters based on artifact and brain signal topographies. *J Clin Neurophysiol*, 2002; 19: 113-24
51. Scarff CJ, Reynolds A, Goodyear BG et al: Simultaneous 3-T fMRI and high-density recording of human auditory evoked potentials. *Neuroimage*, 2004; 23: 1129-42
52. Nuwer MR: Quantitative EEG: I. Techniques and problems of frequency analysis and topographic mapping. *J Clin Neurophysiol*, 1988; 5: 1-44
53. Novitski N, Alho K, Korzyukov O et al: Effects of acoustic gradient noise from functional magnetic resonance imaging on auditory processing as reflected by event-related brain potentials. *Neuroimage*, 2001; 14(1): 244-51
54. Novitski N, Anourova I, Martinkauppi S et al: Effects of noise from functional magnetic resonance imaging on auditory event-related potentials in working memory task. *NeuroImage*, 2003; 20(2): 1320-28
55. Rusiniak M, Lewandowska M, Wolak T et al: A modified oddball paradigm for investigation of neural correlates of attention: a simultaneous ERP-fMRI study. *MAGMA*, 2013; 17: 1-16
56. Jäncke L, Gaab N, Wüstenberg T et al: Short-term functional plasticity in the human auditory cortex: an fMRI study. *Cogn Brain Res*, 2001; 12: 479-85
57. Pluta A, Kurkowski M, Rusiniak M et al: Neural deficits in children with auditory processing disorder. Evidence from functional MRI. *Journal of Hearing Science*, 2011; 1(2): 70-72
58. Bush G, Luu P, Posner MI: Cognitive and emotional influences in anterior cingulate cortex. *Trends Cogn Sci*, 2000; 4: 215-22
59. Hayter AL, Langdon DW, Ramnani N: Cerebellar contributions to working memory. *Neuroimage*, 2007; 36: 943-54
60. Soltani M, Knight RT: Neural origins of the P300. *Crit Rev Neurobiol*, 2000; 14(3-4): 199-224
61. Mulert C, Jäger L, Schmitt R et al: Integration of fMRI and simultaneous EEG: towards a comprehensive understanding of localization and time-course of brain activity in target detection. *Neuroimage*, 2004; 22: 83-94
62. Li Y, Wang L-Q, Hu Y: Localizing P300 generators in high-density event-related potential with fMRI. *Med Sci Monit*, 2009; 15(3): MT47-53
63. Vickery TJ, Jiang YV: Inferior parietal lobule supports decision making under uncertainty in humans. *Cereb Cortex*, 2009; 19: 916-25
64. Andersen RA: Inferior parietal lobule function in spatial perception and visuomotor integration. *Comprehensive Physiology*, 2011; 483-518
65. Radua J, Phillips ML, Russell T et al: Neural response to specific components of fearful faces in healthy and schizophrenic adults. *Neuroimage*, 2010; 49: 939-46
66. Celsis P, Boulanouar K, Doyon B et al: Differential fMRI responses in the left posterior superior temporal gyrus and left supramarginal gyrus to habituation and change detection in syllables and tones. *Neuroimage*, 1999; 9: 135-44
67. Chochon F, Cohen L, Van De Moortele PF, Dehaene S: Differential contributions of the left and right inferior parietal lobules to number processing. *J Cogn Neurosci*, 1999; 11: 617-30
68. Whittingstall K, Stroink G, Gates L et al: Effects of dipole position, orientation and noise on the accuracy of EEG source localization. *Biomed Eng Online*, 2003; 2(1): 14-25
69. Fuchs M, Wagner M, Kastner J: Confidence limits of dipole source reconstruction results. *Clin Neurophysiol*, 2004; 115(6): 1442-51
70. Herrmann CS, Brechmann A, Scheich H: Simultaneous EEG and fMRI of the Human Auditory System In: Mulert C, Lemieux L (eds.), *EEG-fMRI*. Berlin Heidelberg: Springer, 2010; 385-99
71. Karakaş HM, Karakaş S, Özkan Ceylan A, Tali ET: Recording event-related activity under hostile magnetic resonance environment: Is multimodal EEG/ERP-MRI recording possible? *Int J Psychophysiol*, 2009; 73(2): 123-32